

# **SIMULATION ANALYSIS OF IPMSM WITH THREE & FIVE LEVEL DCML INVERTER USING CBSVPWM TECHNIQUE**

***G. Sree Lakshmi, M.Tech***

Associate Professor, Dept of EEE, CVR College of Engineering,  
Hyderabad, Andhrapradesh, India

***S. Kamakshaiah, PhD***

Former Professor, Head & Chairman of Electrical science,  
Dept of EEE, JNT University Ananthapur, Andhrapradesh, India.

***G. Tulasi Ram Das, PhD***

Vice chancellor, JNT University, Kakinada, Andhrapradesh, India.

---

## **Abstract**

In this paper a closed loop controller is designed to obtain the desired output torque, speed and stator phase current of interior permanent magnet synchronous motor (IPMSM) fed by a three & five level diode clamped inverter which is built using IGBTs (Insulated-gate Bipolar Transistors). The modulation technique used is Carrier Based Space Vector Pulse Width Modulation (CBSVPWM). The complex trigonometric calculations involved in conventional SVPWM techniques creates delay in computations and hence the drive response is weakened. Compared to the conventional SVPWM this method is simpler and avoids complex trigonometric calculations and reduced voltage and current harmonics. The model of IPMSM is established in Matlab-Simulink using the equations describing its dynamic behavior. Simulation and analysis is also carried out in Matlab-Simulink.

---

**Keywords:** IPMSM, Three & five level Diode clamped inverter, Carrier Based Space Vector Pulse Width Modulation (CBSVPWM), PI controller

## **Introduction**

Among AC motors, Induction motors are the most preferred one but now-a-days much attention is given to PMSM machines. Permanent Magnet motors are generally AC synchronous machines which operate at unity power factor and are more efficient than induction motor. Initial cost of PMSM are much costly than IM but however due to their higher efficiency

the running cost reduces. With the development of new magnetic materials like Neodymium Iron Boron ( $\text{Nd}_2\text{Fe}_{14}\text{B}$ ) and Samarium Cobalt ( $\text{SmCo}_5$ ) PMSM are becoming more prominent. Permanent magnets provide a constant flux to magnetize the motor. Due to the lack of an electrical magnetization, PMSM gives the advantage of a more energy efficient motor. The use of modern rare-earth magnetic materials enables high flux densities and facilitates the construction of motors with unsurpassed power density (Bimal K. Bose,2009; Marian P. Kazmierkowski, Leopoldo G. Franquelo, Jose Rodriguez, Marcelo A. Perez, and Jose I. Leon,2011; Amor Khlaief, Moussa Bendjedja, Mohamed Boussak,2012).

Depending upon the armature winding distribution PMSM are classified into two types, Brushless DC motors (BLDC) and PMAC. For PMAC machines the armature winding span is close to  $180^\circ$  electrical degrees, which gives the motor a sinusoidal back emf. Whereas the BLDC motors have armature winding span over a smaller angle which gives the motor a trapezoidal shaped back emf. Sinusoidal PMAC machines are classified into two groups with respect to their rotor structures as; Surface Mount Permanent Magnet (SMPM) synchronous motors and Interior Permanent Magnet (IPM) synchronous motors. SMPM motors have the permanent magnets mounted on the outer surface of the rotor, and IPM motors have the permanent magnets buried in the rotor core as shown in Fig.1. IPM motors are newly developed motors with high torque density, high efficiency characteristics and additionally provide field weakening operation, which is impossible with the SMPM motors (Ali Sarikhani, and Osama A. Mohammed,2012; Zhao Kaiqi,2011; Shanshan Wu, David Diaz Reigosa, Yuichi Shibukawa, Michael A. Leetmaa, Robert D. Lorenz, and Yongdong Li,2009). To improve the efficiency and performance of the drive, IPM motors are preferred in the industrial applications because they have the advantage of providing position control loop with accuracy, without a shaft encoder as in case of induction motors. At the end of the 1960s K. Hasses, introduced the field oriented control of AC motor. PMSM can be accurately controlled by using vector control in which field oriented theory is used to control current, voltage and space vectors of magnetic flux. Field oriented control is a basic method in which real- time control of torque variations, rotor mechanical speed and phase currents to avoid current spikes during transient phases is possible (M. Nasir Uddin, Tawfik S. Radwan, G. H. George, and M. Azizur Rahman,2000; L. Zhong, M. F. Rahman,W. Y. Hu, and K. W. Lim,1997; Thomas J. Vyncke, Ren´ e K. Boel and Jan A.A. Melkebeek,2006).

To optimize the drive performance extending the speed range flux weakening control using number of control schemes have been presented. However, drive performance, particularly the torque speed characteristics,

strongly correlates with the employed modulation strategies. The basic modulation technique is a pulse width modulation (PWM) which not only reduces harmonic distortion but also gives constant switching frequency operation of the inverters. After having a detailed survey on various PWM techniques (Jose Rodriguez, Steffen Bernet, Peter K. Steimer, and Ignacio E. Lizama,2010) it is concluded that space vector pulse width modulation (SVPWM) technique gives good performance. SVPWM gives good performance, but however the complexity involved is more in calculating angle and sector. To reduce the complexity involved in SVPWM, a novel modulation technique named Unified voltage modulation or Carrier based space vector pulse width modulation (CBSVPWM) is described using the concept of effective time(Dae-Woong Chung, Joohn-Sheok Kim and Seung-Ki Su,1996; Xiao-ling Wen and Xiang-gen Yin,2007; Jang-Hwan Kim, Seung-Ki Sul and Prasad N. Enjeti,2005).

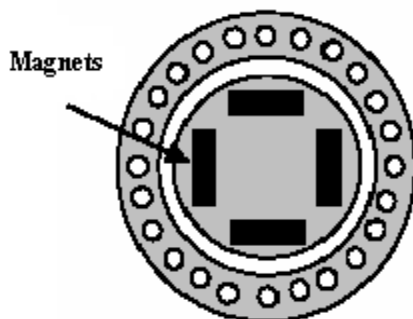


**Fig 1.** Interior permanent magnet motor

By using this method the inverter output voltage is directly synthesized by the effective times and the voltage modulation task can be greatly simplified. The actual gating signals for each inverter arm can be easily deduced as a simple form using the ‘effective time relocation algorithm. To meet medium and high power applications, multilevel inverters are becoming popular(Jose Rodriguez, Jih-Sheng Lai, and Fang Zheng Peng,2002; Nam S. Choi, Jung G. Cho and Gyu H. Cho,1991; J. S. Lai and F. Z. Peng,1996; L. M. Tolbert, F. Z. Peng, and T. Habetler,1999; Leopoldo G. Franquelo, Jose Rodriguez, Jose I. Leon, Samir Kouro, Ramon Portillo, and Maria A. M. Prats,2008). The neutral-point-clamped three-level inverter obtains growing interesting in high voltage and power applications. Compared with the conventional two-level inverter, the three-level inverter has demonstrated significant advantages (Hasegawa.K, Akagi.H, 2012; Ui-Min Choi, Hyun-Hee Lee, and Kyo-Beum Lee, 2013; Chaoying LU, Shuying YANG, Xinfeng WEI, Xing Zhang, 2012). As the level increases, the harmonic content of output voltages and currents can be reduced. In this

paper a three-level & five-level diode clamped inverter fed IPMSM drive has been simulated using CBSVPWM technique. Closed loop torque and speed control is studied using FOC with PI controller.

**Interior Permanent Magnet Synchronous Motor Modelling**

The voltage equation of a synchronous motor on the d-q axis component is represented as given in equation (1). The equivalent circuit of IPMSM in d and q-axes is shown in figure 2.

$$\begin{bmatrix} V_d \\ V_q \end{bmatrix} = \begin{bmatrix} R + pL_d & -\omega L_q \\ \omega L_d & R + pL_q \end{bmatrix} \begin{bmatrix} i_d \\ i_q \end{bmatrix} + \begin{bmatrix} 0 \\ \omega \phi_a \end{bmatrix} \tag{1}$$

Where,

$\phi_a$ : Armature flux linkages due to permanent magnets along the d-axis

$i_d, i_q$ : Armature currents components of d and q- axis

$V_d, V_q$ : Armature voltage components of d and q axis

$L_d, L_q$ : d and q axis inductances

R: Armature winding resistance

p:  $p=d/dt$  Angular Velocity

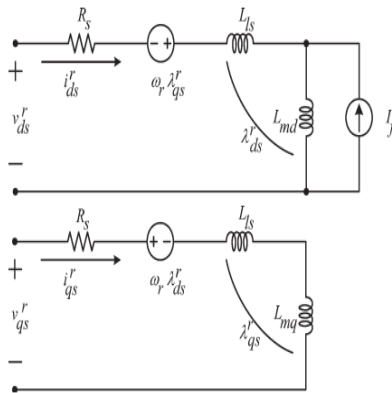


Fig 2. Equivalent circuit of IPMSM in d and q axis

Transforming (1) into  $\alpha - \beta$  fixed coordinate, (2) is derived

$$\begin{bmatrix} V_\alpha \\ V_\beta \end{bmatrix} = \begin{bmatrix} R + pL_\alpha & pL_{\alpha\beta} \\ pL_{\alpha\beta} & R + pL_\beta \end{bmatrix} \begin{bmatrix} i_\alpha \\ i_\beta \end{bmatrix} + \omega_{re} K_E \begin{bmatrix} -\sin\theta_{re} \\ \cos\theta_{re} \end{bmatrix} \tag{2}$$

Where,

$$L_\alpha = L_0 + L_1 \cos 2\theta, \quad L_\beta = L_0 - L_1 \cos 2\theta,$$

$$L_0 = (L_d + L_q)/2, \quad L_1 = (L_d - L_q)/2, \quad L_{\alpha\beta} = L_1 \sin 2\theta \tag{3}$$

An IPMSM is constructed with permanent magnets embedded in the rotor core. This makes the rotor a salient pole and both magnetic torque and reluctance torque can be utilized.

The output torque equation of IPMSM is given by:

$$T = P_n \{ \phi_a i_q + (L_d - L_q) i_d i_q \}$$

$$= P_n \{ \phi_a i_a \cos\beta + 1/2(L_d - L_q) i_a^2 \sin 2\beta \} \quad (4)$$

The output torque T depends on the interlinkage flux  $\phi_a$  and the difference between the d- and q- axis inductance  $L_d - L_q$

Where,

$P_n$  = No. of poles pairs

$I_a$  = Armature current amplitude,

$$I_a = \sqrt{i_q^2 + i_d^2} \quad (5)$$

$\beta$  = Armature current lead angle from the q-axis

The first term in the torque equation (4) represents the magnetic torque generated from the interlinkage flux of the permanent magnets, the second term represents the reluctance torque generated by the differences between d-axis and q-axis inductance.

The motor drive system dynamics is also represented by

$$T_e = T_L + B\omega_m + Jp\omega_m \quad (6)$$

Where  $T_L$  and  $\omega_m$  are load torque and motor speed respectively.

### Control Methods

To run at different speeds, synchronous motors have to be driven by a Variable Frequency Drive (VFD). Electric motors control methods can be divide into two main categories depending of what quantities they control. Scalar Control controls only magnitudes, whereas the Vector Control controls both magnitude and angles. Scalar control is by V/f whereas vector control is possible by Field Oriented control (FOC). Scalar control is the simplest method to control a PMSM, in which frequency is kept constant depending on the speed required and there exist a relationship between voltage and current. No control over angles is utilized, hence the name scalar control. The method uses an open-loop control approach without any feedback of motor parameters or its position. This makes the method easy to implement and with low demands on computation power of the control hardware, but its simplicity also comes with some disadvantages. Vector control allows both magnitude and phase angle control by which higher dynamic performance of the drive system is possible.

### Field Oriented Control (FOC)

The goal of the Field Oriented Control is to control the direct- and quadrature-axis current  $i_d$  and  $i_q$  to achieve required torque. By controlling  $i_d$  and  $i_q$  independently we can achieve a Maximum Torque per Ampere ratio to minimize the current needed for a specific torque, which increases the motor

efficiency. For a non-salient machine, control technique can be easily implemented because  $L_d=L_q$  and produces only one torque i.e electromechanical torque, Whereas for salient machine  $L_d \neq L_q$ , therefore the control is a bit more difficult to implement since the motor produces both electromechanical and reluctance torque. For non-salient pole machine the torque equation is given by

$$T_e = \frac{3P}{2} [\lambda_{pm} I_{sq}] \tag{7}$$

From the above equation the torque producing current is along the quadrature-axis. To reach maximum efficiency, the torque per ampere relationship should be maximum. This can be easily obtained by keeping the direct-axis current to zero at all times. The control systems reference currents  $i_d^*$  and  $i_q^*$  is gives as:

$$i_q^* = \frac{T_e^*}{\frac{3P}{2} \lambda_{pm}} \tag{8}$$

$$i_d^* = 0 \tag{9}$$

For salient pole machine the direct- and quadrature axis inductances are unequal and for the steady state operation the torque equation is given as:

$$T_e = \frac{3P}{2} [\lambda_{pm} I_{sq} - (L_q - L_d) I_{sd} I_{sq}] \tag{10}$$

From the above equation there are two terms affecting the torque production, the electromechanical torque

$$\frac{3P}{2} \lambda_{pm} I_{sq} \tag{11}$$

And the reluctance torque:

$$\frac{3P}{2} (L_q - L_d) I_{sd} I_{sq} \tag{12}$$

**Closed loop PI control using FOC**

The block diagram of closed loop PI control using FOC to investigate the speed and torque control with CBSVPWM for a voltage source three and five-level diode clamped inverter fed IPMSM is presented in fig.3.

Every time the currents and the voltages are measured and transformed into  $\alpha$ - $\beta$  reference frame. The currents are further converted into d-q frame using Park’s Transformation. The reference speed is compared with the motor speed and the error is given to the PI controller. The output of the PI controller is taken as quadrature axis current  $i_q$ . The reference direct-axis current  $i_d = 0$  is considered. The reference direct-axis current is compared with transformed current and given to another PI controller. The output of PI controllers goes to current controller where the voltages  $V_d$  and  $V_q$  can be generated. From these voltages, reference voltages can be generated using CBSVPWM techniques. For generating the pulses for both three and five-level inverters triangular waves are compared with reference

waves. For three-level invert 2 triangular waves are required and for five-level inverter 4 triangular waves are required. Therefore for n-level inverter to generate pulses using CBSVPWM the numbers of triangular waves required are (n-1). The output of the inverter is given to the IPMSM to control the speed and torque of the motor.

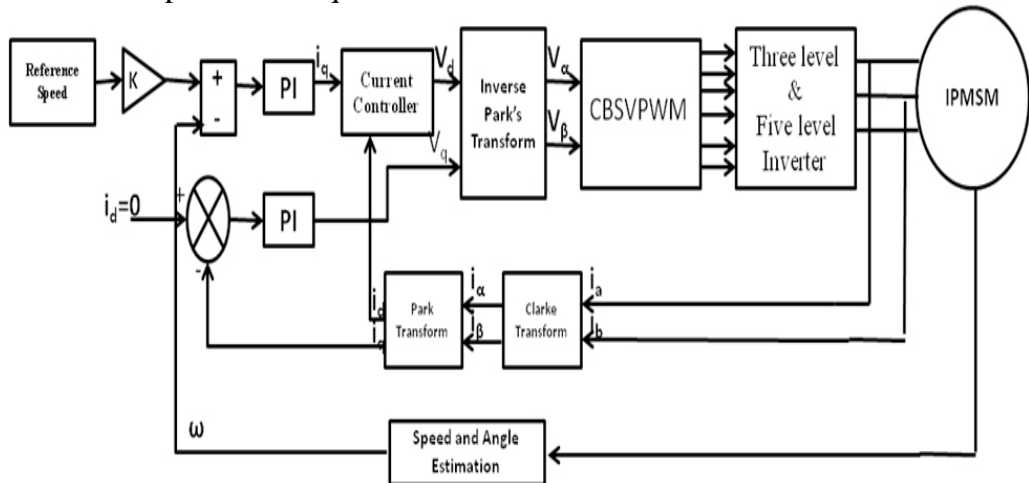


**Fig 3.** Block diagram of closed loop control of three & five-level DCML fed IPMSM using CBSVPWM Technique

### Modulation Techniques

#### Carrier Based Space Vector Pulse Width Modulation

Carrier based SVPWM allow fast and efficient implementation of SVPWM without sector determination. The technique is based on the duty ratio profiles that SVPWM exhibits. By comparing the duty ratio profile with a higher frequency triangular carrier the pulses can be generated, based on the same arguments as the sinusoidal pulse width modulation.

The Fig.4. shows the switching states of sector 1 at different times during two sampling intervals.  $T_s$  denote the sampling time and  $T_{eff}$  denotes the time duration in which the different voltage is maintained.  $T_{eff}$  is called the “effective time”. For the purpose of explanation, an imaginary time value will be introduced as follows:

$$T_{xs} = \frac{T_s}{V_{dc}} V_{xs}^* \quad (x = a, b, c) \tag{13}$$

$V_{as}^*$ ,  $V_{bs}^*$  and  $V_{cs}^*$  are the A-phase, B -phase, and C-phase reference voltages, respectively. This switching time could be negative in the case where negative phase voltage is commanded. Therefore, this time is called the “imaginary switching time”.

Now, the effective time can be defined as the time duration between the minimum and the maximum value of three imaginary times, as given by

$$T_{eff} = T_{max} - T_{min} \tag{14}$$

Where,  $T_{\min} = \min (T_{as}, T_{bs}, T_{cs})$  (15)

$T_{\max} = \max (T_{as}, T_{bs}, T_{cs})$  (16)

When the actual gating signals for power devices are generated in the PWM algorithm, there is one degree of freedom by which the effective time can be relocated anywhere within the sampling interval.

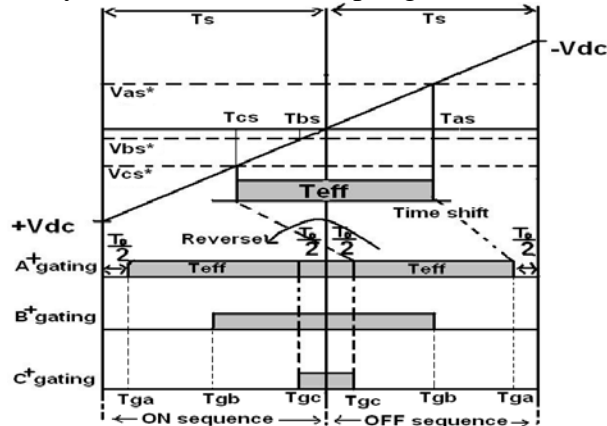


Fig 4. Actual gating time generation for CBSVPWM

Therefore, a time-shifting operation will be applied to the imaginary switching times ( $T_{ga}, T_{gb}, T_{gc}$ ) for each inverter arm, as shown in Fig.4. This task is accomplished by adding the same value to the imaginary times as follows:

$T_{ga} = T_{as} + T_{offset}$  (17)

$T_{gb} = T_{bs} + T_{offset}$  (18)

$T_{gc} = T_{cs} + T_{offset}$  (19)

Where  $T_{offset}$  is the ‘offset time’

This gating time determination task is only performed for the sampling interval in which all of the switching states of each arm go to 0 from 1. This interval is called the “OFF sequence”. In the other sequence, it is called the “ON sequence.” In order to generate a symmetrical switching pulse pattern within two sampling intervals, the actual switching time will be replaced by the subtraction value, with sampling time as follows:

$T_{ga} = T_s - T_{ga}$  (20)

$T_{gb} = T_s - T_{gb}$  (21)

**Three & Five-level diode clamped inverter**

Multilevel inverters are becoming increasingly popular for high power applications, because their switched output voltage harmonics can be considerably reduced by using several voltage levels while still switching at the same frequency. As well, higher input DC voltages can be used since semiconductors are connected in series for multilevel inverter structures, and this reduces the DC voltage each device must withstand. Among the



multilevel topologies, the diode clamped topology has been widely used in which diode is used as the clamping diode to clamp the DC bus voltage so as to achieve steps in the output voltage. In general, the voltage across each capacitor for an n-level diode clamped inverter at steady state is  $V_{dc} / (n-1)$ . The clamping devices have different ratings to produce the voltage of  $V_{dc}/n-1$ . Multiple voltage levels can be provided through connection of the phases to a series of capacitors. For an n-level diode clamped inverter, for each leg  $2(n-1)$  switching devices are required,  $(n-1)*(n-2)$  clamping diodes and  $(n-1)$  dc link capacitors are required.

Figure 5 shows the three-level diode clamped inverter fed to IPMSM drive, where only one DC source  $V_d$  is needed. Two capacitors are used to split the DC voltage and provide a neutral point Z. The inverter leg A is composed of four active switches  $S_{a1}$ ,  $S_{a2}$ ,  $S_{a1}'$  and  $S_{a2}'$  with four anti-parallel diodes  $D_1$  to  $D_4$ . The switches are employed with 12 IGBT's. Switching states for three-level inverter are shown in Table I. For one leg operation of phase-A for a three-level diode clamped inverter, to have a output voltage of  $V_{dc}/2$  the switches  $S_{a1}$ ,  $S_{a2}$  should conduct and to have  $-V_{dc}/2$  voltage, the switches  $S_{a1}'$ ,  $S_{a2}'$  should conduct and to have output voltage as zero the switches  $S_{a2}$ ,  $S_{a1}'$  should conduct. For each voltage level two switches should conduct at a time. The maximum output voltage in the output is half of the DC source.

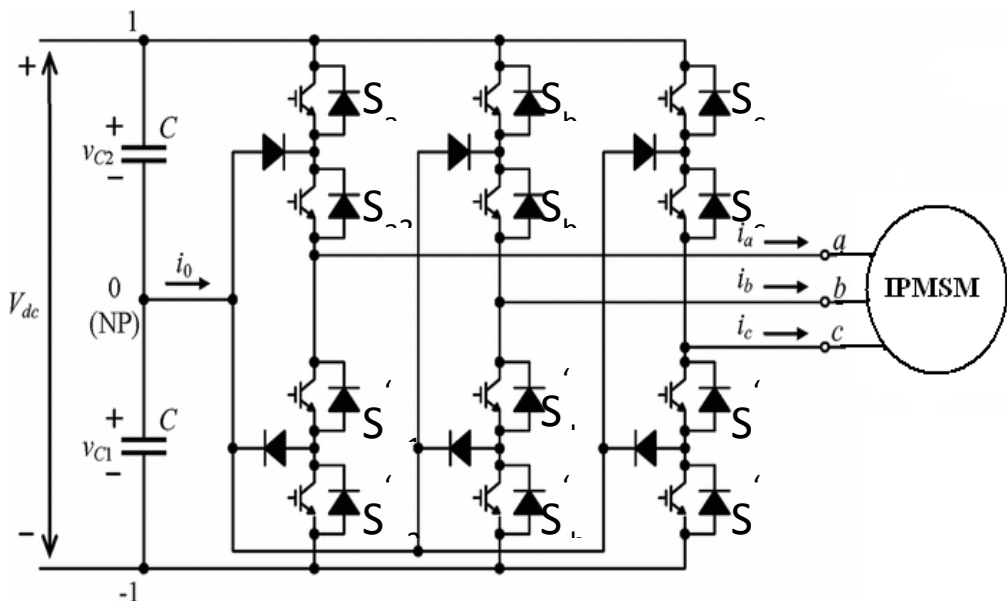


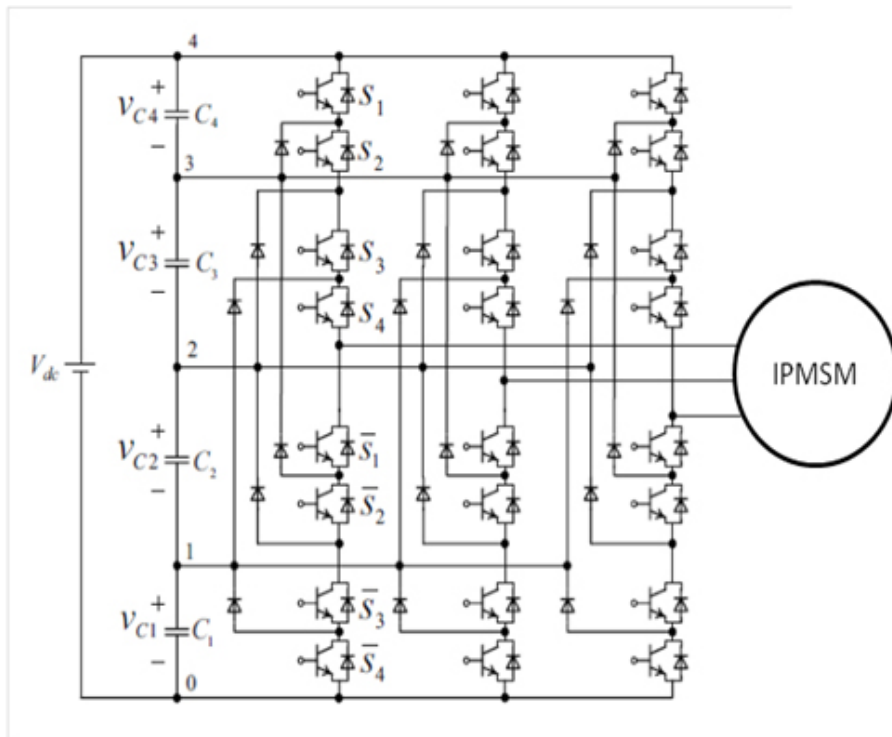
Fig 5. Three-level diode clamped inverter fed IPMSM

Figure 6 shows the five-level diode clamped inverter fed to IPMSM drive, where only one DC source  $V_d$  is needed. Four capacitors are used to

split the DC voltage. The inverter leg A is composed of eight active switches  $S_1, S_2, S_3, S_4, S_1, S_2, S_3$  and  $S_4$  with eight anti-parallel diodes  $D_1$  to  $D_8$ . The switches are employed with 24 IGBT's. Switching states for five-level inverter are shown in Table II. For one leg operation of phase-A, for five-level diode clamped inverter, to have an output voltage of  $V_{dc}/2$  the switches  $S_1, S_2, S_3, S_4$  should conduct, to have  $V_{dc}/4$  voltage, the switches  $S_2, S_3, S_4, S_1$  should conduct, to have zero voltage the switches  $S_3, S_4, S_1, S_2$  should conduct, to have  $-V_{dc}/4$  the switches  $S_4, S_1, S_2, S_3$  should conduct and to have  $-V_{dc}/2$  the switches  $S_1, S_2, S_3, S_4$  should conduct. For each voltage level four switches should conduct at a time. The maximum output voltage in the output is half of the DC source.

**Table 1.** Switching sequences for three-level diode clamped inverter

Output Voltage	Switching Sequence			
	$S_{a1}$	$S_{a2}$	$S_{a1}$	$S_{a2}$
0	0	1	1	0
$V_{dc}/2$	1	1	0	0
$-V_{dc}/2$	0	0	1	1



**Fig 6.** Five-level diode clamped inverter fed IPMSM

**Table 2.** Switching sequences for five-level diode clamped inverter

Output Voltage	Switching Sequence							
	S <sub>1</sub>	S <sub>2</sub>	S <sub>3</sub>	S <sub>4</sub>	S <sub>1</sub> '	S <sub>2</sub> '	S <sub>3</sub> '	S <sub>4</sub> '
V <sub>dc</sub> /2	1	1	1	1	0	0	0	0
V <sub>dc</sub> /4	0	1	1	1	1	0	0	0
0	0	0	1	1	1	1	0	0
-V <sub>dc</sub> /4	0	0	0	1	1	1	1	0
-V <sub>dc</sub> /2	0	0	0	0	1	1	1	1

**Results**

The simulation of the IPMSM electrical drive with three & five-level diode clamped IGBT inverter system is investigated. The control scheme applied for the electrical drive is the field oriented control (F.O.C). The modulation techniques used is CBSVPWM. The system used, was investigated for steady and transient state response. The output waveforms of three phase voltage and current for three & five-level inverter and the torque speed response of three & five level inverter fed IPMSM drive with closed loop FOC is estimated. The parameters used in this simulation are shown in below:

$L_d=0.0066$ ;  $L_q=0.0058$ ;  $R=1.4$ ; PM flux=0.1546;  $P=6$ ;  $F=0.000038818$ ;  $J=0.00176$ ;

Figure 7 (a) & (b) show the reference waveforms of three and five-level inverter using CBSVPWM. Fig.8 (a) & (b) show the reference carrier waveform of three & five-level inverter using CBSVPWM, for three-level two carrier waves are required and for five-level four carrier waves are required to generated the pulses.Fig.9(a) & (b) show the output voltage waveforms of the three & five-level inverter. Fig.10 (a) & (b) show the output current waveforms of the three & five-level inverter.

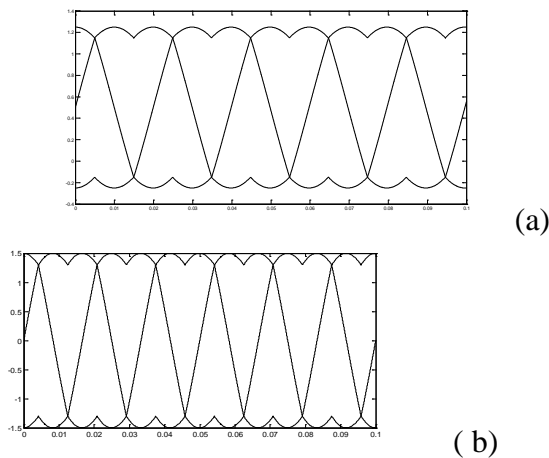


**Fig 7.** Reference waveforms of (a) three-level, (b) five-level diode clamped inverter using CBSVPWM

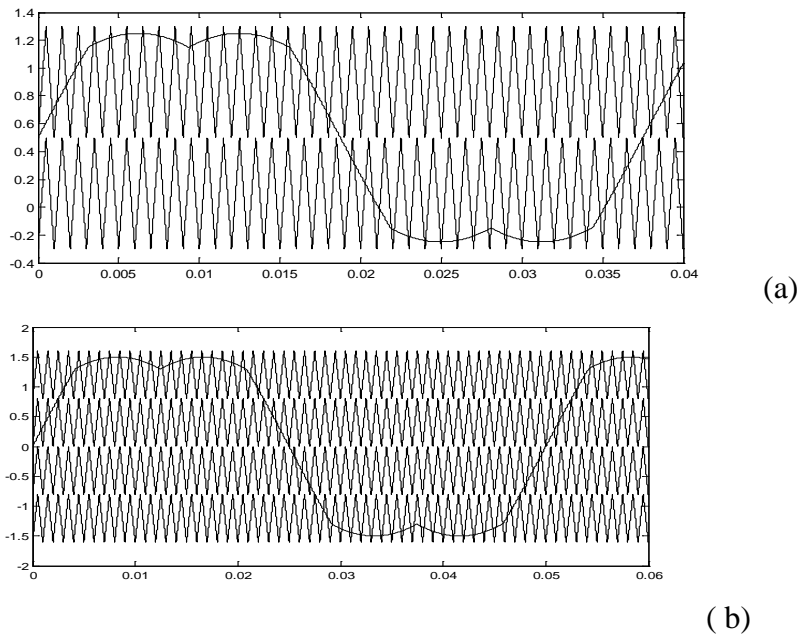


**Fig 8.** Ref\_carrier waveforms of (a) three-level, (b) five-level diode clamped inverter using CBSVPWM

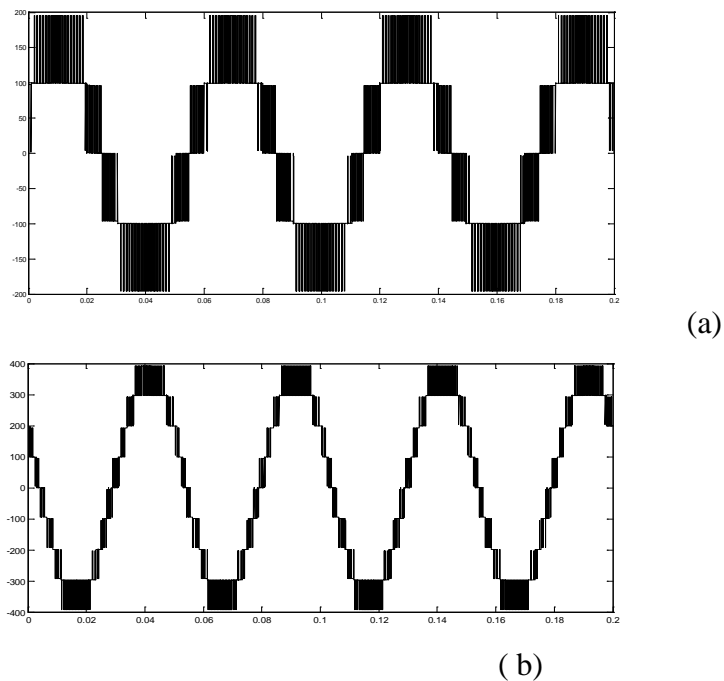
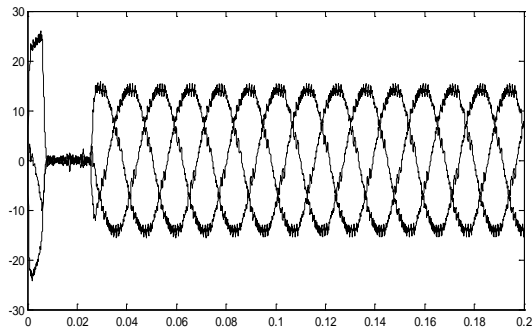
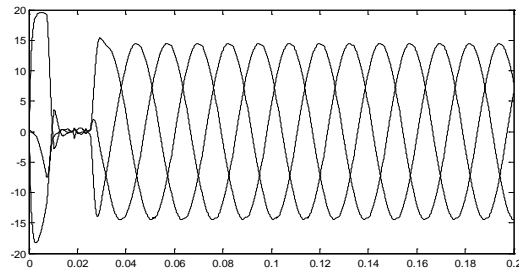


**Fig 9.** Output volatage waveform of (a) Three-level diode clamped inverter using CBSVPWM, (b) Five-level diode clamped using CBSVPWMS

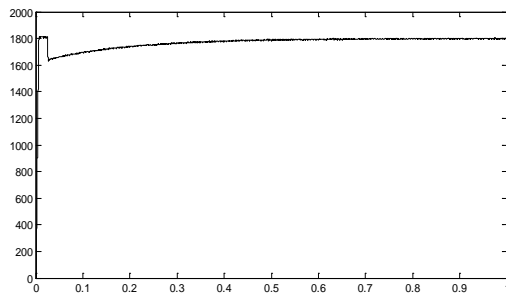


(a)

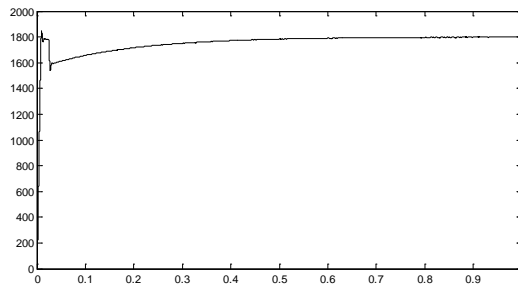


(b)

**Fig 10.** Output current waveform of (a) Three-level diode clamped inverter using CBSVPWM, (b) Five-level diode clamped using CBSVPWM



(a)



(b)

**Fig 11.** Output speed response of (a) Three-level diode clamped inverter fed IPMSM using CBSVPWM, (b) five-level diode clamped using CBSVPWM

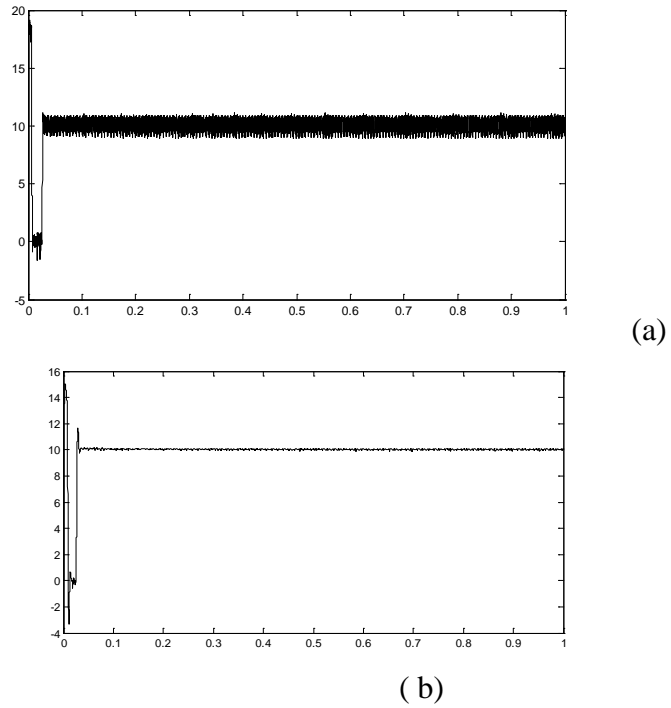


**Fig 12.** Output torque response of (a) Three-level diode clamped inverter fed IPMSM using CBSVPWM, (b) five-level diode clamped using CBSVPWM

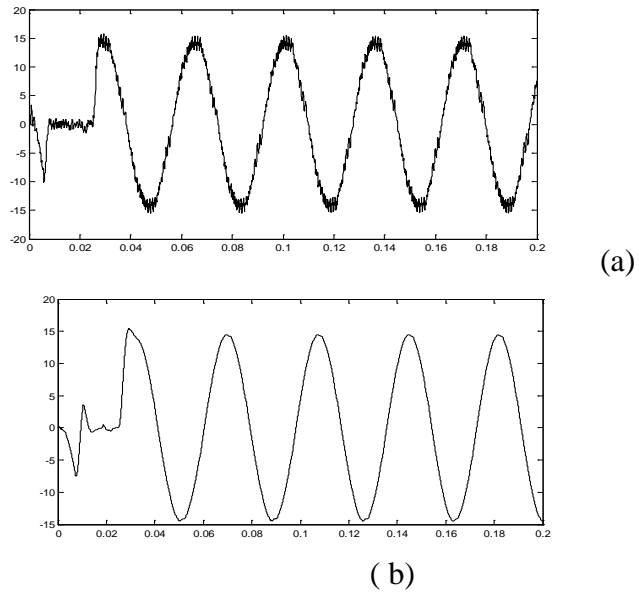


**Fig 13.** Output phase current waveform of (a) Three-level diode clamped inverter fed IPMSM using CBSVPWM, (b) five-level diode clamped using CBSVPWM

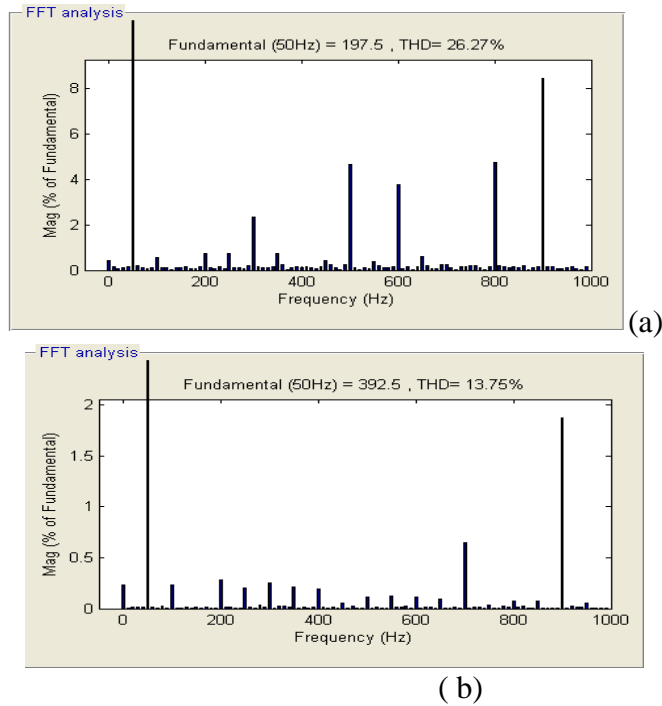


**Fig 14.** THD of output line voltage of (a) three-level diode clamped inverter fed IPMSM using CBSVPWM (b) five-level diode clamped inverter using CBSVPWM

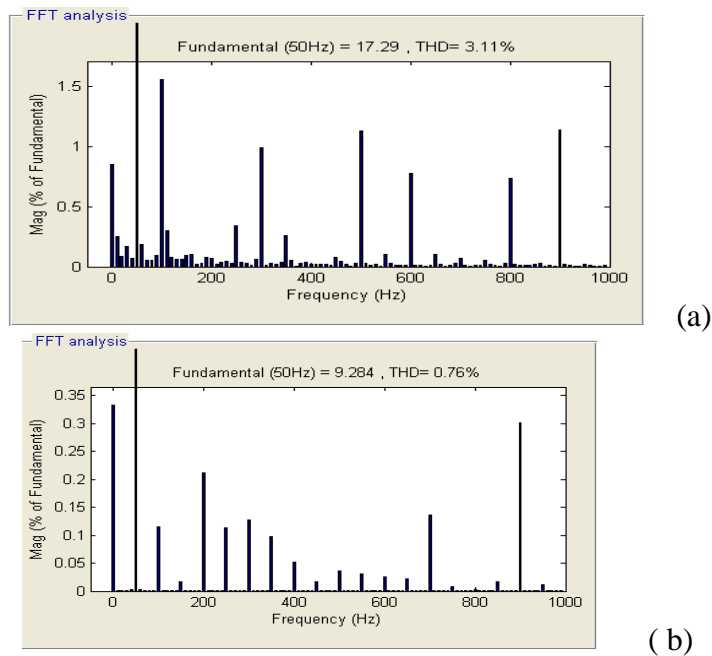


**Fig 15.** THD of output line current of (a) three-level diode clamped inverter fed IPMSM using CBSVPWM (b) five-level diode clamped inverter using CBSVPWM

Figure 11 (a) & (b) shows the output speed response of three & five-level diode clamped inverter fed IPMSM drive using CBSVPWM. Fig.12 (a) & (b) show the output torque response of three & five-level diode clamped inverter fed IPMSM drive using CBSVPWM. Fig.13 (a) & (b) show the output phase current of three & five-level diode clamped inverter fed IPMSM drive using CBSVPWM. Fig.14 (a) & (b) show the THD of output line voltage of a three & five-level diode clamped inverter fed IPMSM using CBSVPWM. Fig.15 (a) & (b) show the THD of output line current of a three & five-level diode clamped inverter fed IPMSM using CBSVPWM. From all the outputs we can conclude that five-level inverter has better performance characteristics compared to three-level inverter.

### Conclusion

In this paper, the simulation model of closed loop control of three & five-level diode clamped inverter fed IPMSM drive using carrier based space vector pulse width modulation (CBSVPWM) techniques has studied. The output voltage, current of the inverter and the speed, torque and the three-phase currents of interior PMSM have plotted. From the analysis we can conclude that the five-level inverter fed IPMSM gives better speed-torque characteristics compared to three-level inverter fed IPMSM with less transients and good steady state response. CBSVPWM is similar to SVPWM but much simple, easy and the fastest method without much mathematical calculations like angle and sector determination as in SVPWM. This method can be easily extended to n-level inverter. From Table.3 the THD of line voltage and line current for five-level diode-clamped inverter is much less than that of three-level inverter.

**Table 3.** Comparison of THD for Three & Five-level DCML Inverter using CBSVPWM

THD	Three-Level Inverter	Five-level Inverter
Line voltage	26.27	13.75
Line current	3.11	0.76

### References:

- Bimal K. Bose, “ Power Electronics and Motor Drives Recent Progress and Perspective,” IEEE Transactions On Industrial Electronics, Vol. 56, No. 2,PP:581-588,2009.
- Marian P. Kazmierkowski, Leopoldo G. Franquelo, Jose Rodriguez, Marcelo A. Perez, and Jose I. Leon,“High-Performance motor drives” IEEE Industrial Electronics Magazine,Vol.5,No.3,PP:6-26,2011.
- Amor Khlaief, Moussa Bendjedia, Mohamed Boussak, “A Nonlinear Observer for High-Performance Sensorless Speed Control of IPMSM Drive,” IEEE Trans. on Power Electronics, Vol. 27, No.6, PP: 3028-3040,2012.



- Ali Sarikhani, and Osama A. Mohammed, “ Sensorless Control of PM Synchronous Machines by Physics-Based EMF Observer,” IEEE Transactions on Energy Conversion, Vol. 27, No.4, PP:1009-1017,2012.
- Zhao Kaiqi, “The Study of Improved PI Method for PMSM Vector Control System Based On SVPWM,” IEEE Conference Publication, PP: 1-4,2011.
- Gilbert Hock Beng Foo, M. F. Rahman, “Direct Torque Control of an IPM-Synchronous Motor Drive at Very Low Speed Using a Sliding-Mode Stator Flux Observer,” IEEE Transactions on Power Electronics, Vol. 25, No. 4, PP:933-942,2010.
- Shanshan Wu, David Diaz Reigosa, Yuichi Shibukawa, Michael A. Leetmaa, Robert D. Lorenz, and Yongdong Li, “ Interior Permanent-Magnet Synchronous Motor Design for Improving Self-Sensing Performance at Very Low Speed,” IEEE Transactions on Industry Applications, Vol. 45, No. 6, PP:1939-1946,2009.
- M. Nasir Uddin, Tawfik S. Radwan, G. H. George, and M. Azizur Rahman, “Performance of Current Controllers for VSI-Fed IPMSM Drive,” IEEE Transaction on Industry Applications, Vol. 36, No. 6, PP: 1531-1538,2000.
- L. Zhong, M. F. Rahman, W. Y. Hu, and K. W. Lim, “ Analysis of Direct Torque Control in Permanent Magnet Synchronous Motor Drives,” IEEE Transactions on Power Electronics, Vol. 12, No. 3, PP:528-536,1997.
- Thomas J. Vyncke, René K. Boel and Jan A.A. Melkebeek, “Direct Torque Control of Permanent Magnet Synchronous Motors – An Overview,” 3<sup>rd</sup> IEEE Benelux young Researchers Symposium in Electrical Power Engineering, Ghent, Belgium,2006.
- Jose Rodriguez, Jih-Sheng Lai, and Fang Zheng Peng, “ Multilevel Inverters: A Survey of Topologies, Controls, and Applications,” IEEE Transactions on Industrial Electronics, Vol. 49, No. 4, PP:724-748,2002.
- Nam S. Choi, Jung G. Cho and Gyu H. Cho, “ A General Circuit Topology of Multilevel Inverter,” IEEE Conference Publication, PP: 96-103,1991.
- J. S. Lai and F. Z. Peng, “Multilevel Converters-A new Breed of Power Converters,” IEEE Transactions on Industrial Application, Vol.32, PP: 509-517, May/June 1996.
- L. M. Tolbert, F. Z. Peng, and T. Habetler, “Multilevel Converters for Large Electric drives,” IEEE Transactions on Industrial Application, Vol.35, PP: 36-44, 1999.
- Leopoldo G. Franquelo, Jose Rodriguez, Jose I. Leon, Samir Kouro, Ramon Portillo, and Maria A. M. Prats, “The Age of Multilevel Converters Arrives,” IEEE Industrial Electronics Magazine, Vol.2, No.2, PP:28-39,2008.
- Jose Rodriguez, Steffen Bernet, Peter K. Steimer, and Ignacio E. Lizama, “A Survey on Neutral-Point-Clamped Inverters,” IEEE Transactions on Industrial Electronics, Vol.57, No.7, PP:2219-2230,2010.

Hasegawa.K, Akagi.H,“Low-Modulation-Index Operation of Five-Level Diode-Clamped PWM Inverter with a DC-Voltage-Balancing Circuit for a Motor Drive,“ IEEE Tansaction on Power Electronics, Vol.27.No.8, PP:3495-3501,2012.

Ui-Min Choi, Hyun-Hee Lee, and Kyo-Beum Lee,“Simple Neutral-Point Voltage Control for Three-Level Inverters Using a Discontinuous Pulse Width Modulation,“ IEEE Transactions on Energy Conversion, Vol.28, No.2, PP: 434-443,2013.

Chaoying LU, Shuying YANG , Xinfeng WEI, Xing Zhang,“Research on the Technology of the Neutral-point Voltage Balance and Dual-loop Control Scheme for Three-level PWM Inverter,“IEEE Conference Publicataion,PP:1-4,2012.

Dae-Woong Chung, Joohn-Sheok Kim and Seung-Ki Sul,“ Unified Voltage Modulation Technique for Real Time Three-phase Power Conversion,“IEEE Transaction,Vol.34,N0.2,PP:374-380,1996.

Xiao-ling Wen and Xiang-gen Yin,“ The Unified PWM Implementation Method for Three-Phase Inverters,“ IEEE Conference Publication,PP:241-246,2007.

Jang-Hwan Kim, Seung-Ki Sul and Prasad N. Enjeti,“ A Carrier-Based PWM Method with Optimal Switching Sequence for a Multi-level Four-leg VSI,“IEEE Conference Publication,PP:99-105, 2005.